Effective generalized predictive control of induction motor

Authors
Patxi Alkorta[1,*], José A. Cortajarena[1], Oscar Barambones[2], Francisco J. Maseda[3]

[1]Engineering School of Gipuzkoa, University of the Basque Country (UPV/EHU), Otaola 29, 20600. Eibar, Spain.

[2]Engineering School of Vitoria, University of the Basque Country (UPV/EHU), Nieves Cano 12, 01006. Vitoria, Spain.

[3]Engineering School of Bilbao, University of the Basque Country (UPV/EHU), Rafael Moreno 3, 48013. Bilbao, Spain.

* Corresponding author:
E-mail address: patxi.alkorta@ehu.eus

Keywords

Generalized Predictive Control (GPC); current and voltage constraints; induction motor; speed and rotor flux control; indirect vector control.

Abstract

In this document it is presented and experimentally validated a new linear predictive regulator to control the mechanical speed and the rotor flux of induction motor (IM). The regulator is developed in the synchronous reference frame and it provides a very good dynamic performance and guarantees fulfilment with the current constraints, to avoid over currents in stator windings. This predictive controller employs the minimum necessary dynamic model of the motor to get minor computational cost, in which the rotor flux and the load torque are estimated, and in spite of important parametric uncertainties, the performance is excellent. Moreover, the predictive regulator anticipates the response and compensates the mechanical dead time of the speed induction motor drive, getting better results than the classic speed PI control scheme. This control scheme incorporates the space vector pulse width modulation (SVPWM) with two proportional-integral (PI) current controllers, where the rest of dynamics of motor (stator) is controlled and voltage constraints are implemented, ensuring that the modulator always works in the linear area, to prevent distortion in the resulting stator currents. From the experimental tests that have been carried out, it can be concluded that the presented controller provides an effective and robust mechanical velocity and rotor flux tracking, from low to high speed range, with a high accuracy.

1. Introduction

The first model-based predictive control (MPC) algorithms emerge in the late 1970's. Several formulations where proposed, where the most popular was the generalized predictive control (GPC), due to its achievement in the regulation of SISO and MIMO industrial systems. The common denominator shared by all these algorithms is based on the model of the system, knowledge of process the future references and thereby provide a control that anticipates the reference changes. This is a benefit respect to the rest of the algorithms, in which only the present and the past samples are considered, without the future ones. In addition, the predictive algorithms ensure a near-optimal working of the system where its constraints have been included in the controller design. Nevertheless, these kind of controllers also involve a disadvantage with respect to classic control approaches because predictive algorithms have a higher computational cost, [1, ch. 1]. Thus, first years the predictive algorithms were employed in slow processes. However, due to technological advances in microprocessors, and especially in the digital signal processors (DSP), predictive algorithms began to be use in other areas where processes are fast as in power electronics.

It is known that predictive control is employed widely in electrical motor drives regulation area, into the power electronics field, with numerous papers in which induction motors have been included. Some of these works have used the GPC to regulate the main variable of the AC motor like position [2], [3], [4] and speed [4], [5]. Nevertheless, other papers have proposed several predictive controllers connected in cascade (Cascade MPC), to regulate the main variable and others, like the rotor flux, the stator currents, replacing the inner PI current regulators by predictive ones, [6], and [7]. Other authors have proposed multivariable predictive solution for mechanical speed and rotor flux as a unique and compact regulator with SVPWM, [8], [9], [10]. At the same time, the predictive current control (PCC) is presented for VSI inverters [11], and a similar algorithm called model predictive torque control (MPTC) is proposed for induction machines [12], where the goal is to replace the inner PI current regulators-PWM set by a predictive current/torque controller, to get faster dynamics with good stator voltage and current total harmonic distortion (THD). Last years, several works, i.e. [13], have presented the cascade predictive

scheme but with PPC in the inner loop.

In spite of that in the recent years exists a trend in research to use more modern AC motors such as PMSM [4], [9] and switched reluctance motors (SRM) [14], [15], the induction motor is still widely used nowadays [3], [13], [16], [17], due to its good characteristics such as small moment of inertia, smooth torque, high initial torque, solid architecture and competitive price. Indirect field oriented control (FOC) or indirect vector control [18], [19], is one of the most known methods used for the induction motor mechanical speed and position control, due to the fact that the torque and rotor flux control references of the induction machine are decoupled, with a minimum ripple in the torque when it uses SVPWM. This modulator offers several advantages respect to the sinusoidal PWM, like best THD index, 15 % higher stator voltage vector for the same DC bus voltage and an easy way to implement digitally due to several low cost microprocessors that incorporate a specific timer to generate this modulation, [20].

The good properties of GPC algorithm applied to regulate main variables (speed, position, rotor flux) of the induction motors can be taken advantage effectively when the future references are known. In this sense, it is necessary to know in detail the dead time of the system in order to be able to anticipate effectively in the control, since otherwise the control will not be anticipative. In practice, pure delays can be found in various types of systems, especially in mechanical, hydraulic and pneumatic systems. Dead time is the delay from when the control signal is applied until the output variable begins to respond or react, [21]. In motor drive systems some interesting research works have been published, in which the dead time of VSI inverter and the computation time have been studied and compensated, getting best THD index and performance of the machine, [22], [23], [24], [25], [26]. But this dead time is small, some units of microseconds. However, none of them have considered the mechanical dead time. The mechanical dead time, referred to the shaft of the electric motor, is much higher than inverter's and computation time's, it can be some hundred microseconds or some units of milliseconds. As a consequence, the dead time of induction motor drive is mainly due to the mechanical part of the induction machine and it can be compensated successfully by using GPC algorithm when it is known.

This paper presents an effective speed and rotor flux GPC regulator, which taking advantage that the

future speed reference and the dead time of induction motor are known, lets to anticipate and to compensate the mechanical dead time of the speed response, getting excellent mechanical speed regulation at low, medium, nominal and very high (flux weakening) speed references. Taking the main ideas of [10] where a unique and compact multivariable GPC regulator is presented, but with the objective to reduce the computational cost of the predictive regulator, because of the fact that the GPC algorithm implies complexity and computational cost, only the minimum necessary dynamics of machine has been taken and transferring the control of the rest of dynamics to other kind of regulators. Thus it is interesting since the predictive controller's benefits can be taken advantage and combined with the properties that other algorithms offer, getting effective and practical cascade regulation schemes. Then taking only two inputs of [10], the mechanical speed and the rotor flux, and avoiding the use of the third input, torque stator current, and its current tracker, a simpler multivariable GPC regulator is obtained and proposed in this paper. The GPC regulator is combined with two PI current controllers and SVPWM, then GPC regulator will be cascaded to the PI-SVPWM scheme. An adequate tuning of stator currents' PI regulators and the symmetric seven vector modulation of SVPWM offer fast dynamics and very low THD in inner loop. In this way, this loop responds quickly to the references of predictive controller. The stator is protected against overcurrents and overvoltages, by constraints imposed to GPC regulator and currents' PI regulators, respectively. As a result, a cascaded GPC-PI controller with excellent fast dynamics, high accuracy, good robustness, with low THD and medium computational cost is obtained. This combination can be an interesting alternative to other predictive algorithm schemes. Section 2 describes the design of GPC controller, in which is also included the design of the speed PI regulator. Section 3 presents a short description of the employed test rig, and several simulation and experimental proves by using the proposed controller. Finally, section 4 shows the obtained conclusions of the paper.

2. Mechanical speed and rotor flux GPC regulator

2.1 Induction motor model

The following differential equations determine the dynamics of the squirrel cage induction motor [18], presented all in the synchronous rotating reference frame *d-q* and supposing that the torque current

component i_{sq} and rotor flux current component i_{sd} are decoupled, that is $\psi_{rq} = 0$ and $\psi_r = \psi_{rd}$

$$T_e - T_L = J\frac{d\omega_m}{dt} + B_v\omega_m \tag{1}$$

$$T_e = \frac{3}{4}p\frac{L_m}{L_r}\psi_{rd}i_{sq} = K_T'\psi_{rd}i_{sq} \tag{2}$$

$$\frac{d\psi_{rd}}{dt} = \frac{R_r}{L_r}L_m i_{sd} - \frac{R_r}{L_r}\psi_{rd} \tag{3}$$

$$v_{sq} = R_s i_{sq} + \sigma L_s\frac{di_{sq}}{dt} + \omega_s\frac{L_m}{L_r}\psi_{rd} + \omega_s\sigma L_s i_{sd} \tag{4}$$

$$v_{sd} = R_s i_{sd} + \sigma L_s\frac{di_{sd}}{dt} + \frac{L_m}{L_r}\frac{d\psi_{rd}}{dt} - \omega_s\sigma L_s i_{sq} \tag{5}$$

The state equations are very appropriate to represent the dynamics of multivariable systems with disturbances, where D is the disturbances matrix

$$\begin{cases}\dfrac{dx}{dt} = A\,x + B\,u + D\,d\\ y = C\,x\end{cases} \tag{6}$$

Thus, replacing Eq. (2) in (1) and taking $\psi_r = \psi_{rd}$, and considering that ψ_r is constant, the differential equations of the induction motor can be presented by using the following state equation based on (1) and (3), where T_L is the load torque measurable (or at least estimable) disturbance

$$\begin{bmatrix}\dfrac{d\omega_m}{dt}\\ \dfrac{d\psi_r}{dt}\end{bmatrix} = \begin{bmatrix}-B_v/J & 0\\ 0 & -R_r/L_r\end{bmatrix}\begin{bmatrix}\omega_m\\ \psi_r\end{bmatrix} + \begin{bmatrix}K_T'\psi_r/J & 0\\ 0 & L_m R_r/L_r\end{bmatrix}\begin{bmatrix}i_{sq}\\ i_{sd}\end{bmatrix} + \begin{bmatrix}-1/J\\ 0\end{bmatrix}T_L \tag{7}$$

and the following output equation

$$\begin{bmatrix}\omega_m\\ \psi_{rd}\end{bmatrix} = \begin{bmatrix}1 & 0\\ 0 & 1\end{bmatrix}\begin{bmatrix}\omega_m\\ \psi_{rd}\end{bmatrix} \tag{8}$$

The rest of dynamics, related with (4) and (5), is controlled by two PI current regulators, as it is explained in [18].

2.2 Mechanical speed and rotor flux GPC regulator design

Since the GPC algorithm uses the discrete version of the state equation, the previous *A*, *B* and *D* matrices must be discretized. In this case the computational method has been employed, then

$$\begin{aligned} A_d &= e^{A\,T_s} \\ B_d &= \int_0^{T_s} e^{A\,\lambda} B\; d\lambda \\ D_d &= \int_0^{T_s} e^{A\,\lambda} D\; d\lambda \\ C_d &= C \end{aligned} \tag{9}$$

where $\lambda = T_s - \tau$ and

$$e^{A\,T_s} \approx I + A\,T_s + \frac{A^2 T_s^2}{2} \tag{10}$$

and if T_s is small, only the first three terms of (10) are considered. It must be noted that the first element of the first row of *B* matrix is variable (due to rotor flux) and in order to use a faithful model of the system, this element is discretized for each sampling period, whereas its value remains constant until the next sampling period. Then, taking into account the commented simplification in (10) and how only an element of *B* matrix must be discretized, the computational effort of the processor is reduced considerably.

The multivariable GPC regulator that is proposed uses the load torque T_L (measurable disturbance), [1, ch. 6],

$$\begin{cases} x(k+1) = A_d x(k) + B_d u(k) + D_d d(k) \\ y(k+1) = C_d x(k+1) \end{cases} \tag{11}$$

where

$$\begin{aligned} x(k) &= \begin{bmatrix} \omega_m(k) & \psi_r(k) \end{bmatrix}^T \\ u(k) &= \begin{bmatrix} i_{sq}(k) & i_{sd}(k) \end{bmatrix}^T \\ d(k) &= T_L(k) \\ y(k) &= \begin{bmatrix} \omega_m(k) & \psi_r(k) \end{bmatrix}^T \end{aligned}$$

Fig. 1 presents the new proposal GPC regulator for the induction motor, where it can be observed that the references imposed to the machine are the mechanical speed and rotor flux. Also it is possible to

observe that the control signals are the stator current linked to electromagnetic torque (consequently to the mechanical speed), i_{sq}*, and the stator current linked to the rotor flux, i_{sd}*, both expressed in the *d-q* rotating reference frame. On the other hand, two PI current controllers are used to convert i_{sq}* and i_{sd}* current commands in their corresponding two v_{sq}* and v_{sd}* voltage commands, which are necessary to get the V_{ABC}^{*} three-phase voltage command to feed the SVPWM modulator.

The design of the GPC regulator uses (11) and follows the procedure detailed in [1, ch. 6] to calculate the output prediction vector equation, which predicts the behaviour of the induction motor in the future along the *N* horizon,

$$\boldsymbol{y} = G\,\boldsymbol{u} + G'u(k-1) + F\,x(k) + F'd(k) \tag{12}$$

$$\boldsymbol{y} = G\,\boldsymbol{u} + \boldsymbol{f} \tag{13}$$

where

$$\boldsymbol{y} = \left[y(k+1+d|k) \quad y(k+2+d|k) \quad \ldots \quad y(k+N+d|k)\right]^T$$

$$\boldsymbol{u} = \left[\Delta u(k) \quad \Delta u(k+1) \quad \cdots \quad \Delta u(k+N_u)\right]^T$$

$$G = \begin{bmatrix} C_d B_d & 0 & 0 & 0 \\ C_d A_d B_d + C_d B_d & C_d B_d & 0 & 0 \\ \cdots & \cdots & \cdots & 0 \\ \sum_{i=0}^{N-1} C_d A_d{}^i B_d + C_d B_d & \cdots & C_d A_d B_d + C_d B_d & C_d B_d \end{bmatrix}$$

$$G' = \begin{bmatrix} C_d B_d \\ C_d A_d B_d + C_d B_d \\ \cdots \\ \sum_{i=0}^{N-1} C_d A_d{}^i B_d + C_d B_d \end{bmatrix} \quad F = \begin{bmatrix} C_d A_d & C_d A_d{}^2 & \cdots & C_d A_d{}^N \end{bmatrix}^T$$

$$F' = \begin{bmatrix} C_d D_d & 0 & 0 & 0 \\ C_d A_d D_d & C_d D_d & 0 & 0 \\ \cdots & \cdots & \cdots & \cdots \\ C_d A_d{}^{N-1} D_d & \cdots & C_d A_d D_d & C_d D_d \end{bmatrix}$$

and where $\boldsymbol{f}$ is the free response component (vector)

$$\boldsymbol{f} = G'u(k-1) + F\,x(k) + F'd(k) \tag{14}$$

The GPC algorithm consists of applying a control sequence that minimizes a J_c multistage cost

function of the form

$$J_c(\boldsymbol{u}) = (\boldsymbol{y} - \boldsymbol{w})^T Q(\boldsymbol{y} - \boldsymbol{w}) + \boldsymbol{u}^T R\, \boldsymbol{u} \tag{15}$$

where the future references of two inputs with a horizon of N are contained in $\boldsymbol{w}$, where d is the dead time of the mechanical part of induction machine

$$\boldsymbol{w} = \begin{bmatrix} \boldsymbol{\omega_m^*} \\ \boldsymbol{\psi_r^*} \end{bmatrix}, \quad \boldsymbol{\omega_m^*} = \begin{bmatrix} \omega_m^*(k+1+d) & \omega_m^*(k+2+d) & \cdots & \omega_m^*(k+N+d) \end{bmatrix}^T \tag{16}$$

$$\psi_r^* = \begin{bmatrix} \psi_r^*(k+1) & \psi_r^*(k+2) & \cdots & \psi_r^*(k+N) \end{bmatrix}^T$$

and where Q is the tracking weighting matrix,

$$Q_m = \begin{bmatrix} \delta_1 & 0 \\ 0 & \delta_2 \end{bmatrix} \tag{17}$$

R is the control weighting matrix,

$$R_m = \begin{bmatrix} \lambda_1 & 0 \\ 0 & \lambda_2 \end{bmatrix} \tag{18}$$

and the incremental control signals are two row vectors, each one consisting of N elements,

$$\boldsymbol{u} = \begin{bmatrix} \Delta i_{sq}^* \\ \Delta i_{sd}^* \end{bmatrix} \tag{19}$$

taking into account that the control horizon is $N_u=1$, and only the first element of each row will be employed.

2.3 Constraints on stator windings

As is well known, the GPC algorithm allows to integrate into the regulator design the control signals constraints. This way, the presented design uses this characteristic to avoid over currents that could damage the stator windings. The following expression relates the three phase currents with the rotor flux and electromagnetic torque currents [18], [19],

$$\vec{i}_s^{\,*} = i_{sd} + i_{sq} j \tag{20}$$

taking from the Table I the nominal value and fixing it as the maximum value of the stator current, $I_{s\,max}$

$= I_{s\,NOM}$, the maximum values are related as

$$I_{s\max} = \sqrt{I_{sd\max}^2 + I_{sq\max}^2} \tag{21}$$

The constraint imposed to the rotor flux current, i_{sd}, is introducing a working margin, i.e., $\Delta i_{sd\max}$, and obtaining the maximum and minimum values or so called constraints,

$$\begin{aligned} I_{sd\max} &= i_{sd} + \Delta i_{sd\max} \\ I_{sd\min} &= i_{sd} - \Delta i_{sd\max} \end{aligned} \tag{22}$$

Regarding the electromagnetic torque current, i_{sq}, its value determines with the rotor flux, the value of electromagnetic torque developed by the motor, (2). This has a direct impact on the value of the three-phase stator currents of the induction motor. Thus, limiting its value, the values of the three phase currents are limited, ensuring the protection of stator windings against over currents. From (21), its value can be calculated as follows,

$$I_{sq\max} = \sqrt{I_{s\max}^2 - I_{sd\max}^2} = -I_{sq\min} \tag{23}$$

There are really two ways to calculate (23). The most sophisticated way using (22), or the simplest way that is used in this design, supposing that the rotor flux has the rated value permanently. So from the steady stationary version of (3) the corresponding current value can be obtained,

$$I_{sd\max} = \frac{\psi_{r\_rated}}{L_m} \tag{24}$$

This part corresponds to two PI current controllers, Fig. 1. The design of these current regulators is done in the frequency domain, choosing their band-width with the gain cross-over frequency, ω_{ci} , and the phase margin, PM_i , as it is described in [18]. When for the tandem SVPWM modulation-VSI are employed the vector control techniques, it is necessary to limit the module of the phase stator voltage reference vector to work in the linear area of the modulator, [18]. This value is determined by the DC bus voltage of the inverter, according to the following expression

$$\left|\vec{v}_s^{\,*}\right|_{\max} = \frac{V_{DC}}{\sqrt{3}} \tag{25}$$

whereas it is known, the voltage vector is made up by the direct and quadrangular components

$$\vec{v}_s^{\,*} = v_{sd} + v_{sq} j \tag{26}$$

and it must comply

$$\sqrt{v_{sd}^2 + v_{sq}^2} \leq \frac{V_{DC}}{\sqrt{3}} \tag{27}$$

Thus, if the module of voltage, $\left|\vec{v}_s^{\,*}\right|$, is higher than maximum (25), then both components of this vector must be scaled or reduced proportionally (multiplying its component by $\left|\vec{v}_s^{\,*}\right|_{\max}$ and dividing by $\left|\vec{v}_s^{\,*}\right|$). This is implemented in *Lim* block in Fig. 1.

2.4 Estimation of θ_s , ψ_r and T_L load torque

The θ_s angle is necessary to implement the Park's transformation, which is calculated by using the indirect vector control method and for that it is necessary to integrate the ω_s synchronous speed,

$$\omega_s = \omega_{slip} + \omega_r \tag{28}$$

being ω_{slip} the slip speed and ω_r the electrical rotor speed. The ω_m mechanical rotor speed is employed to calculate the electrical rotor speed,

$$\omega_r = \omega_m \frac{p}{2} \tag{29}$$

Taking into account the assumptions adopted in the beginning of this section, that is, $\psi_{rq} = 0$, $d\psi_{rq}/dt = 0$ and $\psi_r = \psi_{rd}$, the slip speed is calculated by using (30)

$$\omega_{slip} = \frac{L_m}{\psi_r} \frac{R_r}{L_r} i_{sq} \tag{30}$$

The rotor flux, ψ_r, is easily estimated using (3) and supposing $\psi_r = \psi_{rd}$.

The load torque is the part of the estimable disturbance that is calculated using equation (1) in which is previously included (2)

$$\hat{T}_L = K_T' \psi_{rd} i_{sq} - J \frac{d\omega_m}{dt} - B_v \omega_m \tag{31}$$

2.5 GPC regulator tuning

The tuning of the GPC controller needs to choose two horizons (minimum, N_1 , and maximum, N_2) and two weighting factors (λ_1 and λ_2). N is the prediction horizon and defines the number of the GPC regulator's coefficients (size of G and $\boldsymbol{f}$). In this way, higher value for N increases the anticipative effect, getting better control and system's performance, but on the other hand, there is an increase in the number of coefficients and the computational cost of the regulator, and consequently, an increase in the sampling period. Thus, N has been chosen to get a good dynamic performance and a medium-low computational cost, so in this design the selected value is $N=5$. The minimum and maximum horizons take into account the delay time of the system [1], $N_1=1+d$, and, $N_2=N+d$. The sample time choosen for all controllers is 100 μs (VSI inverter at 10 kHz), and the offline experimentally measured delay time at different operation states of the mechanical part of the induction motor is around 700 μs, (subsection 3.2). Then, the delay value is 7 sampling periods that is, $d=7$, and consequently $N_1=6$ and $N_2=12$. Anyway, the delay time must be always a multiple of the sampling time.

Decreasing the control weighting factor, λ, the response of the controlled system is faster. Increasing the tracking weighting factor, δ, the same result is obtained. A simple and effective way to tune this regulator is fixing to unity the tracking weighting factors δ_1 and δ_2, and selecting only λ factors, applying the following empirical equations to get the optimal values for λ_1 and λ_2 (trace() gets the sum of the diagonal elements of the matrix in brackets),

$$\lambda_1 = trace\left(G_1^T G_1\right),\ \lambda_2 = trace\left(G_2^T G_2\right) \qquad (32)$$

It must be noted that G matrix depends only on the plant (induction motor) parameters, and it is a multivariable system, being 2Nx2N matrix (10x10). This way, it can be obtained G_1 , that is, the mechanical speed part of G, (NxN, formed by G's odd columns) and G_2 , the rotor flux part (NxN, formed by G's pair columns).

However, in spite of the mechanical speed and rotor flux tracking is good in simulation tests, control signals may be overly aggressive, especially in real experiments. In these cases, it is recommended to use a gain K to smooth the control signal. Increasing this gain, the control signal is smoother.

Table II corresponds to the speed-rotor flux GPC regulator designs, where D1 is the ideal or nominal case taking into account the rated parameters values of the machine (Table I). D2 is the case which takes uncertainties in mechanical parameters (J, B_v) when their values are 3 times lower than its nominal values. D2A takes the uncertainty only in J, D2B takes only in B_v , and D2C takes the parameter uncertainties in both at same time, Table II 3rd , 4th and 5th columns, respectively. Regarding D3, this case takes uncertainties in mechanical parameters (J, B_v) when their values are 3 times higher than its nominal values. D3A takes the uncertainty only in J, D3B takes only in B_v , and D3C takes the parameter uncertainties in both at same time, Table II 6th , 7th and 8th columns, respectively. According to the commented in the previous paragraph, when the resulting λ_1 is much lower than in the nominal case, K has to be higher than the nominal value to get more smooth control signal (60, in cases D3A and D3C). However, when the obtained λ_1 is much higher than in the nominal case, K has to be lower than nominal value to get a softer control signal (1, in cases D2A and D2C).

2.6 PI regulators tuning

As is well known, in this proposal the GPC regulator is connected to two current PI regulators (GPC-PI), and consequently it implies that these regulators must be adjusted as fast as possible. Both regulators use the same tuning values and the adjusted parameters are obtained using frequency domain technique, [18]. With the selection of the bandwidth and the phase margin, the values of kp_{is} and ki_{is} are obtained. Selecting a higher bandwidth for the controllers improves the dynamic performance of the currents loops. Nevertheless, any real system has its physical limit to the bandwidth. For the experimental platform employed (subsection 3.1), this limit is located around 3500/4000 rad/s; for higher values the platform generates dangerous mechanical vibrations that can damage the machine. In this way, to ensure a fast response of PI current regulators and work at safe frequency, a bandwidth of ω_{ci} = 3000 rad/s with a margin phase of PM_i =1.5707 rad (90º) has been chosen. With this phase margin the faster response without any overshoot for this bandwidth is obtained. This is the D1 design in Table III, it is the ideal or nominal case taking into account the rated parameters' values of the machine (Table I). Regarding D2R design in Table III, this case takes 31.2 % less than real for R_s and R_r , and it is implemented to

demonstrate the robustness of electrical part o the motor related to the resistances (stator and rotor) when they are at 100º C. The parameters of the controllers are designed with rotor and stator resistances (R_r and R_s) 31.2% less than really are in the experiment (as a consequence R_r and R_s would be working at an equivalent temperature of 100 ºC), (33).

$$R_f = R_0\left(1+\alpha\ (T_f - T_0)\right) \tag{33}$$

A speed PI regulator is implemented to measure the mechanical delay time of the induction motor and to compare the designed GPC regulator results with this classic controller. This speed PI regulator is also designed employing the frequency domain technique, but due to method requirements, using a bandwidth 10 times smaller than the two current PI regulators, [18]. Thus, D1 design is the nominal case in Table IV and it takes $\omega_{c\omega}$ = 300 rad/s with a margin phase of PM_ω =1.4311 rad (82º) is designed. With this phase margin the faster response with minimum overshoot for this bandwidth is obtained. This way, this speed PI regulator connected to the two current PI regulators provide a good PI speed regulator for induction motor. Regarding mechanical parameters uncertainties, two designs have been presented. D2C and D3C, corresponding with D2C and D3C of Table III, respectively.

3. Results of simulation and experimental proves

3.1 Test bench

The employed test rig is based on the M2AA 132M4 ABB commercial induction motor of 7.5 kW of die-cast aluminium squirrel-cage type and 1445 rpm described in Table I, which is connected to three-phase VSI inverter with a DC bus of 540 V. The induction motor receives the load torque in its shaft from a 10.6 kW 190U2 synchronous motor. The control and monitoring unit is made up by a Personal Computer with the DS1103 real time target dSpace (PowerPC processor to 1 GHz), its monitoring application dsControl and the simulation environment MatLab/Simulink. The test rig includes several sensors: three half effect sensors to measure the three-phase stator currents, and an incremental encoder of 4096 pulses with a FPGA module to measure the mechanical speed. The SVPWM modulator/VSI inverter works with a constant switching frequency of 10 kHz, this way the sample time

utilized for the multivariable GPC and PI current regulators, and also for speed PI regulator, is the minimum possible, that is 100 μs.

Due that this GPC algorithm includes control signals constraints, the linear solution of the minimization cost function (15) is not valid, [1, ch.7]. As a consequence, a nonlinear optimization method must be employed, where in this proposal the Truncated-Newton bound constrained (TNC) is used. In this sense, the minimization cost function (15) has been implemented by using the *tnc()* function, in both in simulation and in experimental tests. The *tnc()* function has been written in C programming language [27] by using a Simulink's S-Builder Function block to implement the designed GPC multivariable regulator. Moreover, the maximum number of iterations that it uses for the numerical solution can be programmed. Certainly, all tests have been done setting its value to 5 iterations, which is the minimum value necessary to reduce the computational cost while the best performance is guaranteed.

3.2 Mechanical speed and rotor flux tracking (D1 design)

This subsection shows the performance of the machine for D1 design (Table II and III) by using several simulation and experimental tests. A trapezoidal speed reference of 1000 rpm / 0.5 Hz and a rotor flux reference with two constant values over 10 s are employed for this. Note that in second part of tests, the rotor flux reference takes its nominal (Table I), starting at 5.25 s. Moreover, the load torque is gradually increasing: it is null throughout the first 3 s, a constant of 10 N·m up to 4.5 s, ±25 N·m square form between 4.5-7.5 s, and ±40 N·m square form between 7.5-10 s. Figure 2 shows the simulation test, in which it can be observed that the tracking of the obtained speed tracking is very acceptable in quantity and quality, graph (a), where the error steady-state is approximately 1-2 rpm (0.1-0.2 %), graph (b). In the first part of the test (0-3 s), the load torque or disturbance is null and consequently the rotor flux value (d) can be lower than nominal to get an excellent speed tracking. But when the load torque appears, the rotor cannot track properly the speed reference and the speed error is increasing a lot (3.5-4.5 s), due that the rotor flux is not sufficiently big to generate the necessary electromagnetic torque (2), although the torque current has its maximum value (c). To overcome the load disturbance's effect, starting from 6 s, the rotor flux reaches the imposed reference nominal value and after this instant the machine is able to keep a very

good speed tracking, as the initial part of the test, obtaining newly an error steady-state around 1-2 rpm. To get it, the stator current associated to rotor flux is increased in a step way from 4.013 A to 8.026 A (e). Note that the reference value generated by this GPC controller is into the limits imposed for i_{sd} current constraints (Table II) and according to (22) they are 8.025 - 8.027 A, and that the real value is very similar to the reference getting a very good rotor flux current tracking. As a consequence, the rotor flux tracking is also very satisfactory, graph (d). Moreover, it can be noted that the torque current neither exceed its maximum and minimum values (± 20 A) imposed as a current constraints, graph (c), and consequently the stator current is also limited, as it is shown in graph (g). Graph (f) exhibits the electromagnetic or motor torque developed by the induction machine and the requested and estimated load torque in its shaft, where it can be appreciated that the motor torque is very effective but at the same time smooth, and the high similarity between the real and estimated load torques. In the (h) graph the module of the stator voltage vector in *d-q* synchronous rotation frame is showed, in which it is observed that its value does not exceed its maximum value (311 V), (25), Table II. Finally, graph (i) displays the quantity of iterations employed by the *tnc()* minimization cost function (between 2 and 5).

Figure 3 shows the experimental test corresponding to the simulation test shown in Figure 2. Comparing the graphs between both tests, we can see that the experimental test gets practically the same waveforms respect to its simulation case, where the speed error steady-state is a bit higher, that is 2-5 rpm (0.2-0.5 %). Consequently, the proposed GPC regulator is validated experimentally, getting very good speed and rotor flux tracking in spite of the presence of load disturbance.

Figure 4 shows a comparative between GPC and PI regulators employing the same experimental test than in Figure 3. Two cases have been considered for PI regulators, with and without feed-forward estimated load torque term. It should be noted that PI regulator works better with feed-forward term, getting faster and better response than without it. As it can be seen, the GPC controller gets the most rapid and robust (in presence of load torque) speed response: its response has the lowest overshoot and stabilizes earlier than the PI regulators. Graphs (b) and (c) show how the GPC response is faster than the PI regulators due to the anticipative effect. Figure 5 shows the performance comparison between GPC

and PI regulators, employing a square speed reference waveform of 600 rpm and 0.5 Hz. Observing PI regulator's response in graph (a), it can be seen that it has a mechanical delay time of 7 sampling times; that is, it is delayed 0.0007 s (700 μs, d=7) respect to the speed reference. This is the time interval that the motor needs since the torque current reference changes, in 4 s instant, (b). However, the GPC regulator compensates the delay time and anticipates 5 steps (N), generating the control signal 12 steps before (N_2) than the PI case.

Figure 6 shows the experimental test based in the previous Figure 3, but working in nominal conditions: the speed reference and the load disturbance take the nominal values (Table I) in the last part of the test (7.5-10 s). In this way, it is possible to test the benefits of the proposed GPC regulator working in rated conditions. It is possible to observe in the first part of the test, in which the rotor flux is weak (0-6 s), that the speed tracking is very good for constant speed reference, but when the reference is increasing or decreasing, exists an important speed error (b) and the speed tracking is not so good (a). However, in the second part of the test (6-10 s), when the rotor flux is nominal, the speed tracking is excellent, obtaining a steady-state speed error less than 5 rpm (0.346 %). It is interesting to remark, that the rotor flux (d) and its current (e) tracking are as good as the previous test (Figure 3), and the electromagnetic torque (f) is also smooth and effective. Finally, it can be observed that the stator current (c, g) and voltage (h) are not overcome the nominal values imposed as constraints in the design of the presented regulator. Figure 7 compares the last experimental test employing GPC regulator (Figure 6) with the same test employing PI regulator. As it can be seen, both speed responses are good, however the GPC regulator gets better speed tracking than PI controller.

Figure 8 shows the experimental test in which in its first part (0-5.5 s) the speed reference's maximum value is higher than motor's rated value (2000 rpm), (a), while the rotor flux is lower than rated value (flux weakening regimen), (d), as in the previous cases. Moreover, a square form load disturbance of 10 N·m is also applied (1.5-6 s), (f). As can be observed, the speed tracking is very satisfactory in the first part, obtaining a steady-state speed error lower than 5 rpm (0.25 %), (b). The second part starts with a step speed reference of 160 rpm and with the rated value for rotor flux reference.

In this case, an increasing (-10 to 30 Nm) square form load disturbance is also applied. Taking into account these adverse conditions (low speed and high load), it can be considered that the obtained speed tracking is very good, where the speed error is lower than 1 rpm (0.625 %). Next, another step of 600 rpm is applied to the motor and the load torque changes (30 to -40 N·m), medium speed and high load, obtaining excellent result with a speed error around 1 rpm (0.166 %). Finally, last step of 1400 rpm is required to the machine, with a square load torque of ± 40 N·m, getting a speed error lower than 3 rpm (0.214 %). Moreover, the rotor flux and its current tracking are very satisfactory along the test, graphs (d) and (e) respectively, and the electromagnetic torque is smooth and effective (f). On the other hand, the current and voltage constraints are not exceeded in any moment of the test, graphs (c)-(g) and (h), respectively.

Figure 9 compares these results with the same test done using the PI regulator, observing the four different speed zones of the probe. Graph (a) shows that at -2000 rpm with weak rotor flux and low load torque, the GPC regulator's response is faster than the PI case at speed reference changes and load changes, nevertheless the PI controller has a slightly better performance in the second part (4.1-4.8 s). Graphs (b) and (c) confirm that the GPC regulator's response is faster than the PI and also that the GPC controller's response stabilizes before than the PI when the load torque changes sharply. Finally, graph (d) also confirms the two previous affirmations, and also, shows that while GPC regulator offers very good speed tracking in all moment, PI controller's response can not track properly the reference in some intervals of time (8.9-9.5 s).

3.3 Mechanical speed and rotor flux tracking (D2 and D3 designs for robustness demonstration)

This subsection shows the experimental test's performance for D2 and D3 designs (Tables II and III). For that, the previous experimental test showed in Figure 3 has been used. First is analysed the performance of the induction machine controlled by GPC regulator taking into account the mechanical parameter uncertainties (J, B_v) when their values are 3 times minor than real ones (Table II). Figure 10 shows the comparative for D1, D2A, D2B and D2C designs' responses. As can be seen, all of GPC designs' results are very similar to nominal case (D1), getting very good performance in all cases in spite

of important parameter uncertainties, with a speed error minor than 2 rpm (0.2 %). For get these results, and according to commented in the last paragraph of subsection 2.5, the gain *K* has been adjusted to get the best results in the cases in which the moment of inertia (*J*) is different than real one (D2A, D2C). As the moment of inertia is minor than nominal case (real), the resulting λ_1 control factor is much higher than in the nominal case, then to compensate it *K* has to be lower, getting more control action (more aggressive), taking the value 1. The variation of viscous coefficient (B_v) has not any effect on resulting λ_1 (D2B), then *K* keeps the nominal value, 3.5. See in the last row, third, fourth and fifth columns.

Second, it is studied the performance of the induction motor regulated by GPC regulator taking into account the mechanical parameter uncertainties (*J*, B_v) when their values are 3 times higher than real ones. In Figure 11 can be seen the comparative for D1, D3A, D3B and D3C designs' responses. It can be observed that the results referred to D3A and D3C are worse than D1 and D3B, due that error is higher (about 5 rpm, 0.5 % vs. 2 rpm, 0.2 %), but in general they are good taking into account the important parameter variations. As the moment of inertia is higher than nominal case (real), the resulting λ_1 control factor is much lower than in the nominal case (D3A, D3C). As a consequence, the control action is very aggressive and to smooth it, *K* has to be higher than nominal case, taking the value 60. The viscous coefficient (B_v) variations almost has not any effect on resulting λ_1 (D3B), then *K* maintains the nominal value, 3.5. See in the last row, sixth, seventh and eighth columns. Then, the compensation of higher moment of inertia using the gain *K* is worse than lower inertia case, and consequently the results (speed error) are also worse.

Finally, Figure 12 shows the experimental test taking D2C (mechanical part) and D2R (electrical part) setup, and adding measurement white noise in the ω_m rotor speed and i_{sA} stator current feedback signals, In this way, robustness of the presented regulator against parameter uncertainties, load disturbances and measurement noises is demonstrated. Taking (a) and (b) graphs, it is possible to observe that in spite of all adversities, the speed tracking is very good, obtaining a speed error around 15 rpm (1.5 %). Moreover, the rotor flux tracking is also very good (c) and the electromagnetic torque generated by the motor is effective and quite smooth, taking into account the important value of noises (d). Regarding

the stator current, really it is limited to constraint value but it contains the added noise and it is the expected value that overcomes the current constraint because it is added externally out of the GPC regulator (e). Anyway, clearly the current keeps its maximum value around the current constraint (20 A). Moreover, the stator voltage (f) value is into the limit imposed by the voltage constraints (311 V). Figure 13 shows the comparative performance of the GPC regulator with the same experimental test employing the PI controller. In this figure can be seen that the speed tracking is very similar for both, however, the GPC response is a bit faster than the PI.

4. Conclusions

This research work presents a novel multivariable linear GPC controller for squirrel cage induction motor, which regulates effectively the mechanical rotor speed and the rotor flux. Due that the GPC algorithm implies complexity and computational cost, only the minimum necessary dynamics of machine has been taken and transferring the control of the rest of dynamics to PI regulators. The design is based on the reduced-order linear state equations of the machine, where the nonlinear term related to the load torque is located in the measurable disturbance term. The current loops and the VSI inverter control are regulated using the standard PI-SVPWM tandem, obtaining very good harmonics index in stator currents and being as an excellent industrial solution. The predictive regulator incorporates the stator currents constraint, while the voltage constraint is located in PI currents controllers. The regulator employs estimated physical variables such as rotor flux and load torque, and also measured variables like mechanical rotor speed and stator currents. This predictive control proposal takes into account the mechanical dead time of the induction motor in its design and provides a very satisfactory and robust mechanical velocity and rotor flux tracking in both favourable and unfavourable circumstances (load torque, important parametric uncertainties and measurement noise in feedback signals). The experimental results have demonstrated its better robustness, a faster speed response and a faster stabilization compared with the traditional speed PI control scheme. It is important to note that if the delay time is increased and it is not compensated, when the machine is asked for high dynamics such in machine tool and robotics sectors, unacceptable tracking errors will occur. Thus, the induction motor works perfectly

with different amplitudes for speed and rotor flux independently each of the other, including both the very high speed, nominal, medium and low speed zones, getting very high dynamics and accuracy; less than 0.346 % speed error for nominal case, and around 1.5 % for adversities case. All the experimental tests that have been carried out provide an experimental validation of the presented rotor speed-flux GPC controller. Moreover, taking into account that only one of the motor dynamics terms must be discretized in each sampling time and that the maximum number of iterations for *tnc()* minimization function is set to 5, the computational cost of this regulator is around 60 μs with a floating- point PowerPC processor to 1 GHz, around 15 % less than the proposed in [10]. Taking into account these all benefits offered by this GPC proposal, this control scheme could be adequate to be used in industrial applications. Moreover, this novel GPC regulator could be employed with other different current regulators instead of PI ones, getting other cascade schemes, or including without any current regulator by using a hysteresis modulator.

Acknowledgements

The authors wish to express their gratitude to the Basque Government through the project SMAR3NAK (ELKARTEK KK-2019/00051), to the Diputación Foral de Álava (DFA) through the project CONAVAUTIN 2, to the Gipuzkoako Foru Aldundia (GFA) through the project ETORKIZUNA ERAIKIZ 2019 and the UPV/EHU for supporting this research work.

References

[1] E. F. Camacho and C. Bordons, *Model Predictive Control*. Springer-Verlag London Limited, 2nd Ed, 2004, ch. 1, 6 & 7.

[2] P. Alkorta, O. Barambones, J. A. Cortajarena, "Linear Generalized Predictive Position Control of Induction Motor Drives", *Proc. 37th Annual Conf. of the IEEE Ind. Electron. Society*, pp. 1922–1927, Melbourne, 2011.

[3] W. A. Silva, A. B. S. Junior, B. C. Torrico, D. A. Honório, T. R. Fernandes, L. N. dos Reis, L. H. S. Barreto, "Generalized Predictive Control Robust for Position Control of Induction Motor using Field-Oriented Control" *Springer-Verlag Berlin Heidelberg*, vol. 97, no 3, pp. 195–204, Jan. 2015.

[4] K. Belda, D. Vošmik, "Explicit Generalized Predictive Control of Speed and Position of PMSM Drives" *IEEE Trans. Ind. Electron.*, vol. 63, no 6, pp. 3889–3896, Jun. 2016.

[5] K. Belda, D. Vošmik, "Speed Control of PMSM Drives by Generalized Predictive Algorithms", *Proc. 38th Annual Conf. of the IEEE Ind. Electron. Society*, pp. 2012–2017, Montreal, 2012.

[6] R. Hedjar, P. Toumi, P. Boucher and D. Dumur, “Cascaded Nonlinear Predictive Control of Induction Motor”, *European Journal of Control*, vol. 10, no. 1, pp. 65-80, 2004.

[7] S. Chai, L. Wang and E. Rogers, “A Cascade MPC Control Structure for a PMSM with Speed Ripple Minimization” *IEEE Trans. on Industrial Electronics*, vol. 60, no. 8, pp. 2978-2987, Aug. 2013.

[8] E. Souza de Santana, E. Bim and W. Caradori do Amaral. “A predictive algorithm for controlling speed and rotor flux of induction motor”. *IEEE Trans. Ind. Electron.*, vol. 55, no. 12, pp. 4398-5518. Dec. 2008.

[9] S. Chai, L. Wang, and E. Rogers, “Model predictive control of a permanent magnet synchronous motor with experimental validation”, *Control Engineering Practice*, vol. 21, no. 11, pp. 1584–1593, Nov. 2013.

[10] P. Alkorta, O. Barambones, J.A. Cortajarena and A. Zubizarreta, “Efficient Multivariable Generalized Predictive Control for Sensorless Induction Moto Drives”. *IEEE Trans. Ind. Electron.*, vol. 61, no. 9, pp. 5126-5134. Sep. 2014.

[11] J. Rodríguez, J. Pontt, C.A. Silva, P. Correa, P. Lezana, P. Cortés and U. Amman, “Predictive Current Control of a Voltage Source Inverter”, *IEEE Trans. Ind. Electron.*, vol. 54, no. 1, pp. 495-503, Feb. 2007.

[12] H. Miranda, P. Cortés, J. I. Yuz and J. Rodríguez, “Predictive Torque Control of Induction Machines Based on State-Space Models”, *IEEE Trans. Ind. Electron.*, vol. 56, no. 6, pp. 1916-1924, Jun. 2009.

[13] C. García, J. Rodríguez, C. Silva, C. Rojas, P. Zanchetta and H. Abu-Rub, “Full Predictive Cascaded Speed and Current Control of an Induction Machine”, *IEEE Trans. Energy Conv.*, vol. 31, no. 3, pp. 1059-1067, Sep. 2016.

[14] T. Turnisi, M. Villani, G. Fabri and L. Di Leonardo, “A switched-reluctance motor for aerospace application: Design, analysis and results”, *Electric Power Systems Research*, vol. 142, pp. 74–83, Jan. 2017.

[15] J. Shao, Z. Deng and Y. Gu, “Sensorless Control for Switched Reluctance Motor based on special position detection”, *ISA Trans.*, vol. 70, pp. 410–418, Aug. 2017.

[16] N. Pimkumwong and M-S. Wang, “Full-order observer for direct torque control of induction motor based on constant V/F control technique”, *ISA Trans.*, vol. 73, pp. 189–200, Feb. 2018.

[17] Y. Guven and S. Atis, “Implementation of an embedded system for real-time detection of rotor bar failures in induction motors”, *ISA Trans.*, vol. 81, pp. 210–221, Oct. 2018.

[18] N. Mohan, *Advanced Electric Drives*, Mineapolis, USA, MNPERE Mineapolis, 2001, ch. 5.

[19] B. K. Bose, *Modern Power Electronics and AC drives*, Knoxville, USA, Prentice Hall, 3rd ed, 2002, ch. 8.

[20] N. V. Kumar, P. A. Michael, J. P. John and S. S. Kumar, “Simulation and comparison of SPWM and SVPWM control for three phase inverter”, *ARPN Jour. Of Eng. and Applied Sciences*, vol. 5, no. 7, pp. 61–74, Jan. 2010.

[21] B. C. Kuo, *Automatic Control Systems*, New Jersey, USA, John Wiley & Sons, 8th ed, 2003, ch. 4.

[22] Chul-Woo Park and Woo-Hyen Kwon, “Time-delay compensation for induction motor vector control system”, *Electric Power Systems Research*, vol. 68, pp. 238–247, Mar. 2004.

[23] A. Guha and G. Narayanan, "Delay Compensation in Model Predictive Control of a Three-Phase Inverter", *IEEE Trans. on Industrial Electronics*, vol. 59, no. 2, pp. 1323-1325, Feb. 2012.

[24] M. Uddin, S. Mekhilef, M. Nakaoka and M. Rivera, "Model Predictive Control of induction motor with delay time compensation: an experimental assessment", *Proc. IEEE Applied Power Electronics Conf. and Expositionl*, pp. 543-548, New Orleans (USA), 2015.

[25] T. Abhiram, P. V. N. Prasad and P. S. Reddy, "Integrated Dead-Time SVPWM algorithm for Indirect Vector Controlled Two-level Inverter fed Induction Motor Drive", *Proc. IEEE Int. Conf. on Information, Communication, Instrumentation and Control*, paper Id: 182, Indore (India), 2017.

[26] A. Guha and G. Narayanan, "Impact of Undercompensation and Overcompensation of Dead-Time Effect on small-Signal Stability of Induction Motor Drive", *IEEE Trans. on Industry Applications*, vol. 54, no. 6, pp. 6027-6041, Dec. 2018.

[27] J.-S. Roy, "TNC: a non linear optimization package", web publication: http://js2007.free.fr/code/index.html, 2004.

Tables

Notation	Value
P_N nominal power	7.5 kW
V_N nominal voltage	380 V
$T_{e\ NOM}$ nominal electromagnetic torque	50 N·m
R_s stator resistance	0.729 Ω
R_r rotor resistance	0.40 Ω
L_m magnetizing inductance	0.1125 H
L_s stator inductance	0.1138 H
L_r rotor inductance	0.1152 H
P number of poles	4
J moment of inertia (nominal)	0.0503 kg·m^2
B_v viscous friction coefficient (nominal)	0.0105 N·m/(rad/s)
$\omega_{m\ NOM}$ nominal mechanical speed	151.32 rad/s (1445 rpm)
$V_{s\ NOM}$ nominal stator voltage (rms)	380 V
$I_{s\ NOM}$ nominal stator current (rms)	15.24 A
$I_{sq\ NOM}$ nominal torque current	20 A
$I_{sd\ NOM}$ nominal rotor flux current	8.026 A
$\Psi_{r\ NOM}$ nominal rotor flux	0.9030 Wb
α, temperature coefficient Al/Cu	0.0039 K^{-1}

Table I. Induction motor parameters

Parameter	D1	D2A (J/3)	D2B (B_v/3)	D2C (J/3 B_v/3)	D3A (J3)	D3B (B_v3)	D3C (J3 B_v3)
J	0.0503	0.0168	0.0503	0.0168	0.1509	0.0503	0.1509
B_v	0.0105	0.0105	0.0035	0.0035	0.0105	0.0315	0.0315
λ_1	2.9e-3	2.61e-2	2.9e-3	2.61e-2	3.22e-4	2.9e-3	3.22e-4
λ_2	1.6e-7	1.6e-7	1.6e-7	1.6e-7	1.6e-7	1.6e-7	1.6e-7
$I_{sq\ max}$	20 A	20 A	20 A	20 A	20 A	20 A	20 A
$\Delta i_{sd\ max}$	0.001 A	0.001 A	0.001 A	0.001 A	0.001 A	0.001 A	0.001 A
K	3.5	1	3.5	1	60	3.5	60

For all designs: $N=5$, $d=1$, $N_u=1$, $\delta_1=1$, $\delta_2=1$

Table II. Speed and Rotor flux GPC regulator designs

Parameter	D1	D2R
R_s	0.729	0.5556
R_r	0.40	0.3048
ω_{c_isq}	3000 rad/s	3000 rad/s
PM_{isq}	90º	90º
ω_{c_isd}	3000 rad/s	3000 rad/s
PM_{isd}	90º	90º
kp_{isq}	11.81	11.81
ki_{isq}	2187	1666.9
kp_{isd}	11.81	11.81
ki_{isd}	2187	1666.9
$\|v_s\|_{max}$	311 V	311 V

Table III. Current PI regulators designs

Parameter	D1	D2C (J/3 B_v/3)	D3C (J3 B_v3)
ω_{c_ω}	300	300	300
PM_ω	82	82	82
J	0.0503	0.0168	0.1509
B_v	0.0105	0.0035	0.0315
kp_ω	5.64	1.88	16.94
ki_ω	238.17	79.39	714.51

Table IV. Speed PI regulator designs

Figures

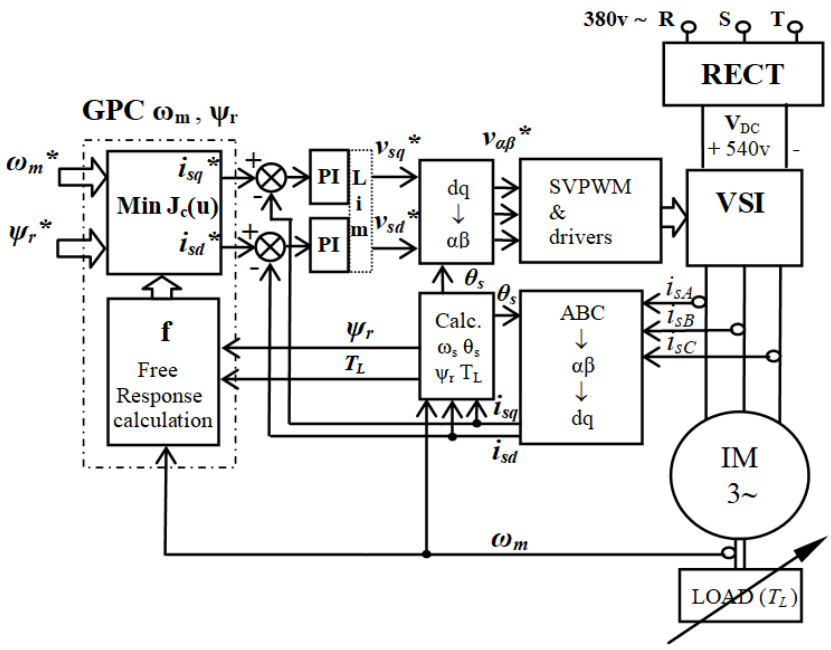

Figure 1: Blocks scheme of the presented mechanical speed and rotor flux GPC controller for induction motor.

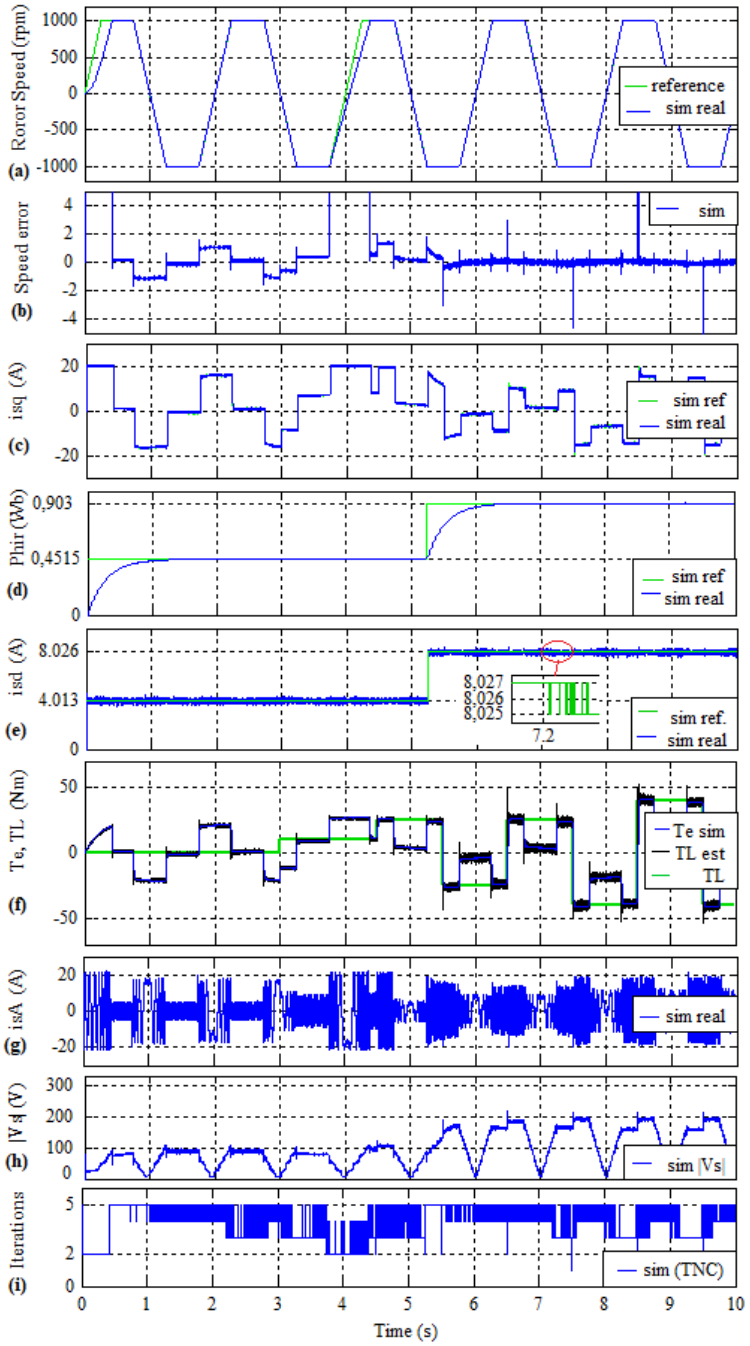

Figure 2: Simulation prove of the GPC regulator for induction motor, D1 design.

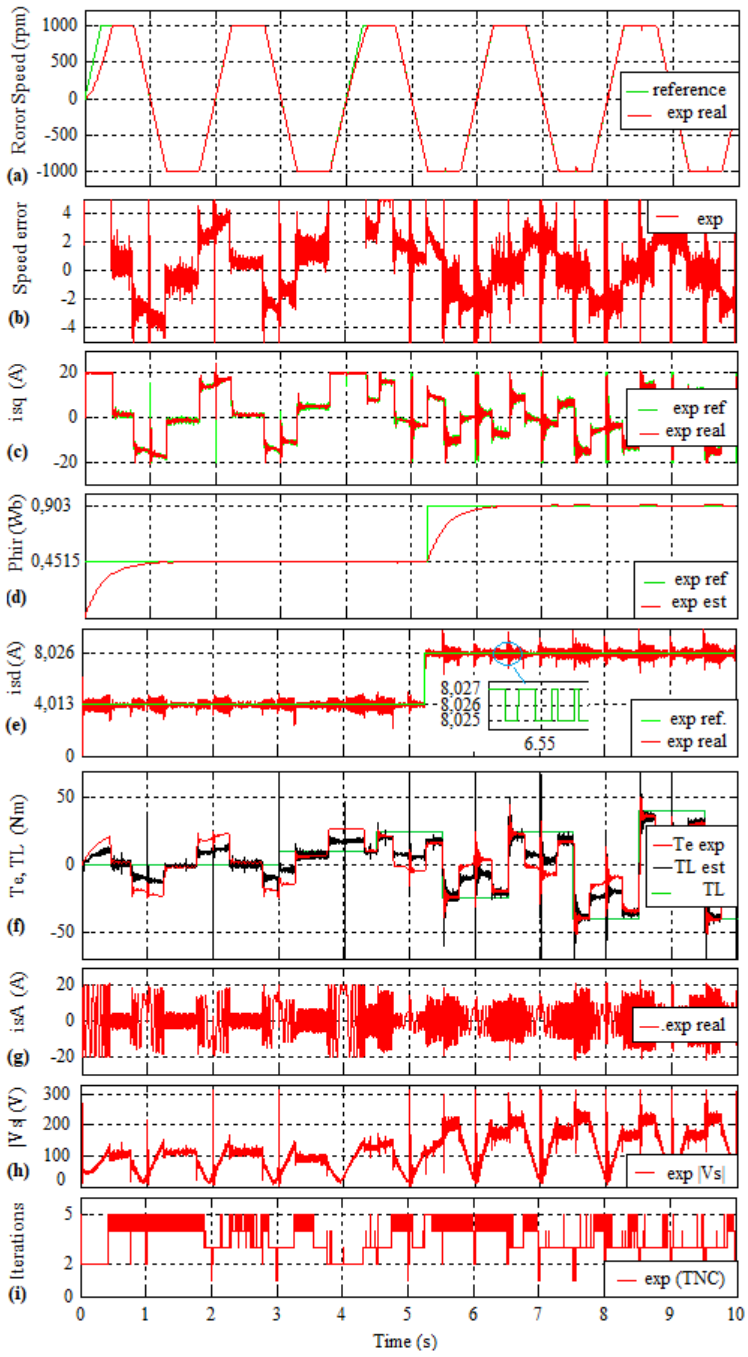

Figure 3: Experimental prove of the GPC regulator for induction motor, D1 design.

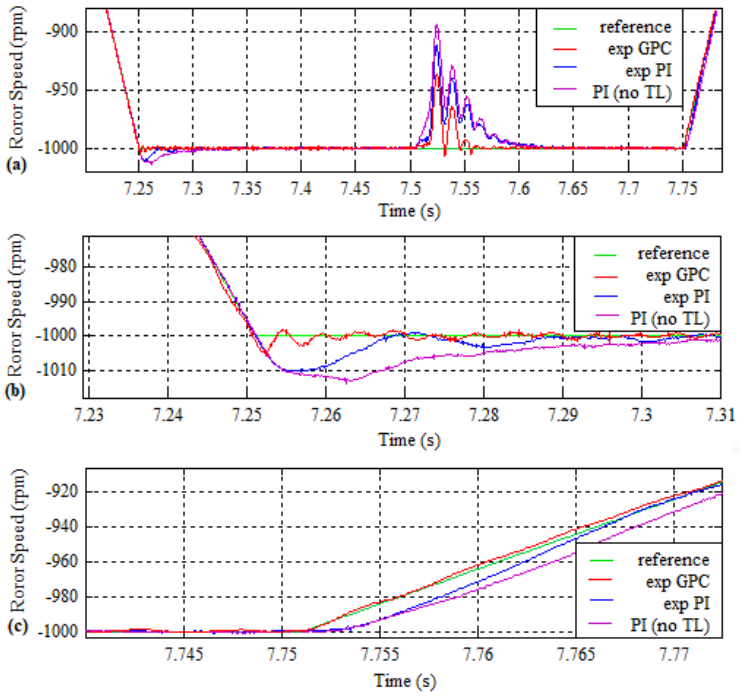

Figure 4: Experimental tests for performance comparison between the GPC and the PI regulators for induction motor, D1 design.

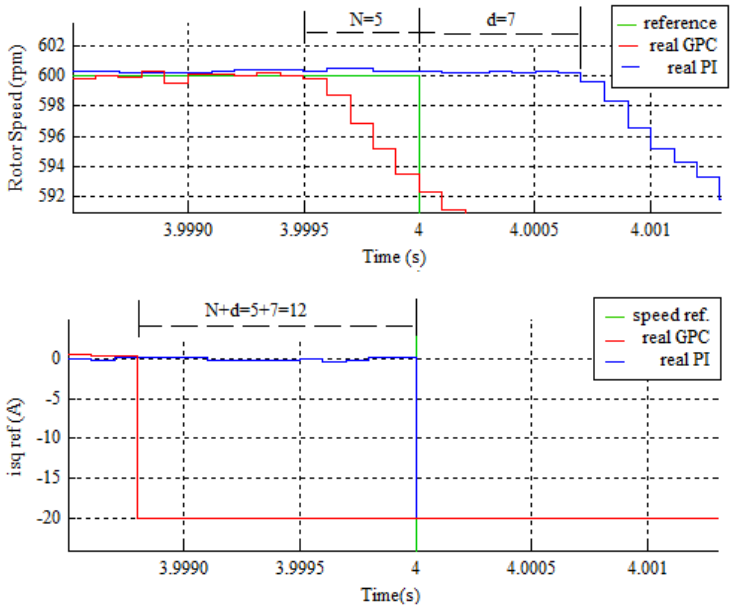

Figure 5: Experimental tests for performance comparison between the GPC and the PI regulators for induction motor, D1 design.

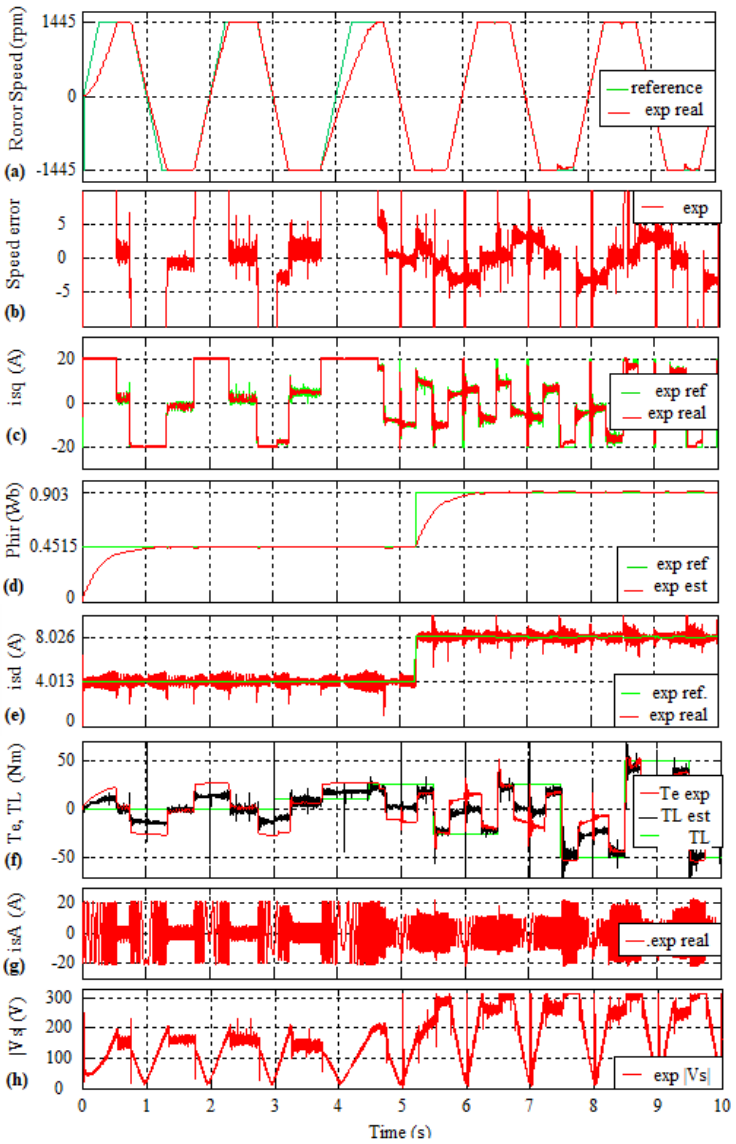

Figure 6: Experimental test of the GPC regulator for induction motor working in nominal conditions, D1 design.

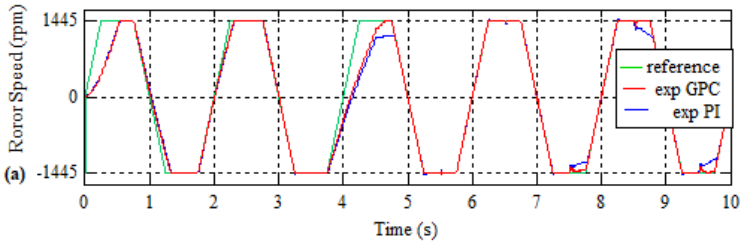

Figure 7: Experimental tests for performance comparison between the GPC and the PI regulators for induction motor in nominal conditions, D1 design.

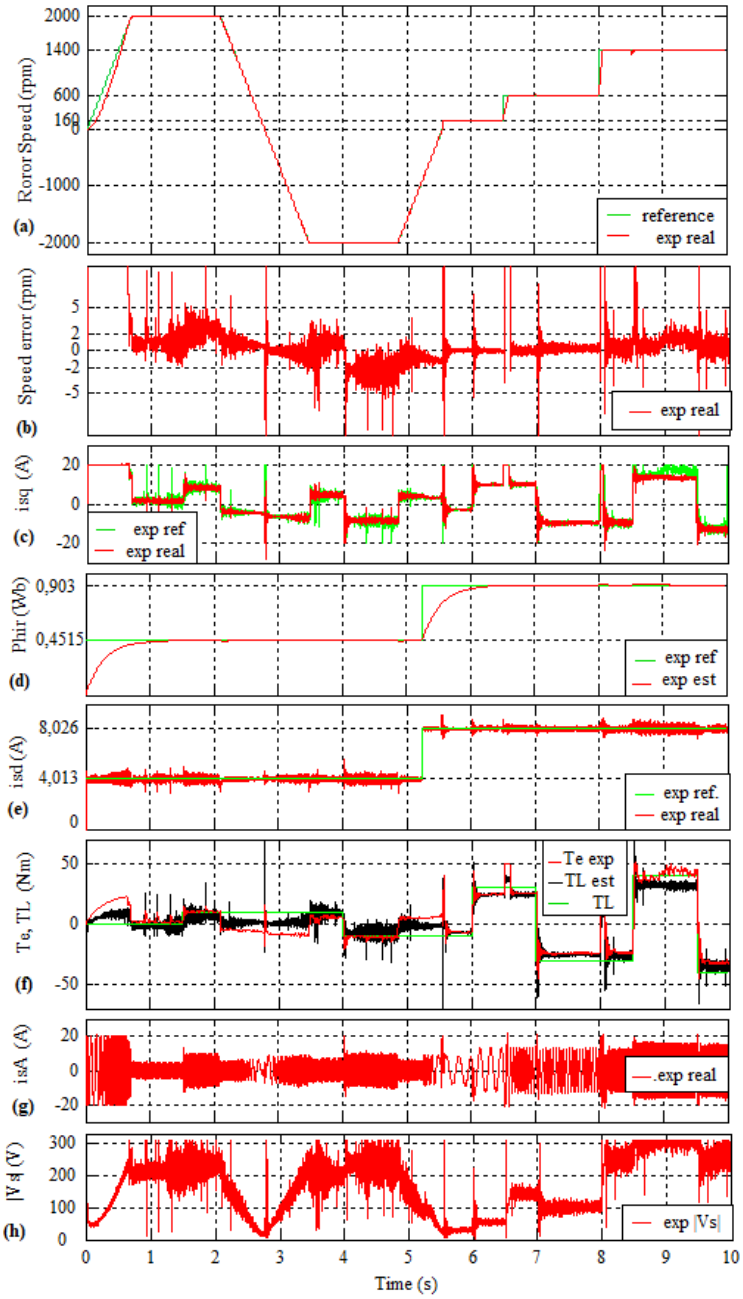

Figure 8: Experimental test of the GPC regulator for induction motor at very high, low and medium speed, D1 design.

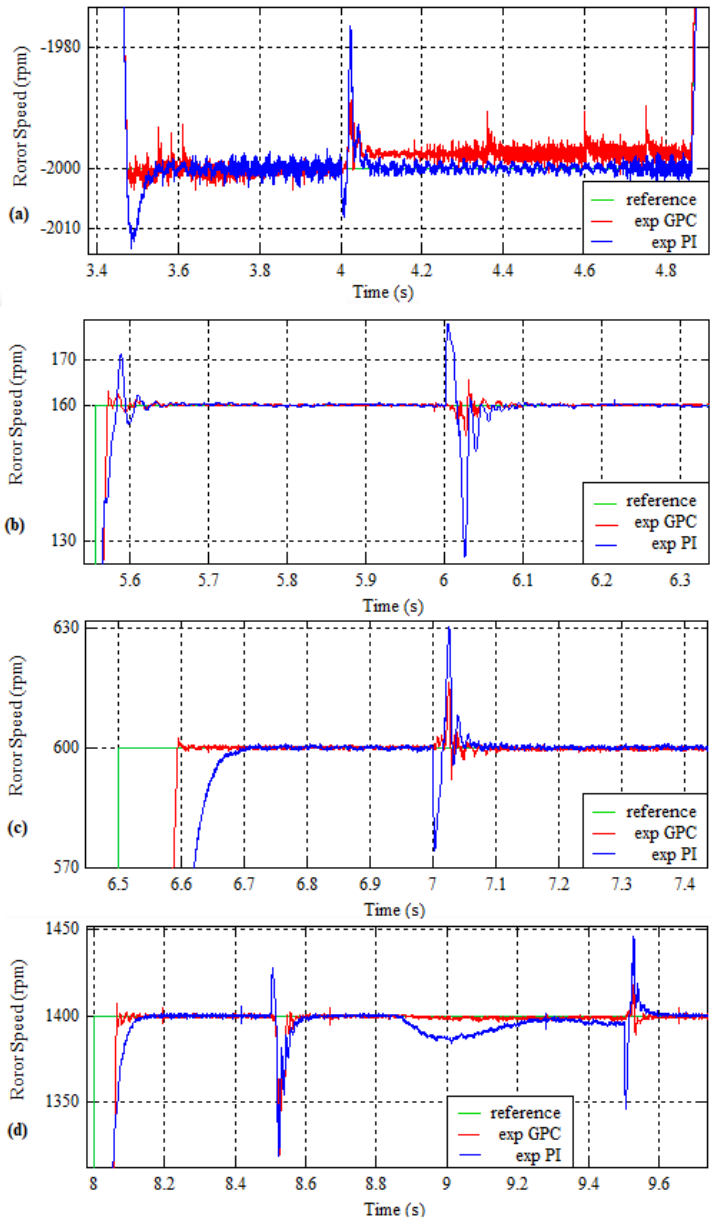

Figure 9: Experimental tests for performance comparison between the GPC and the PI regulators for induction motor at very high, low and medium speed, D1 design.

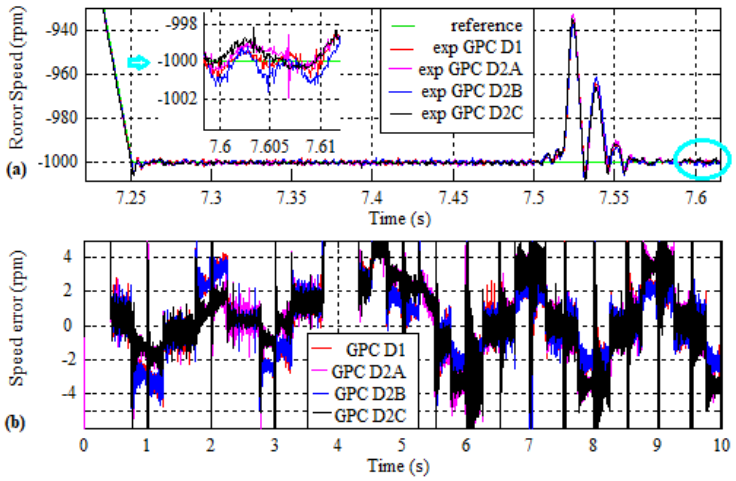

Figure 10: Experimental tests for performance comparison between D1, D2A, D2B and D2C, GPC controller designs.

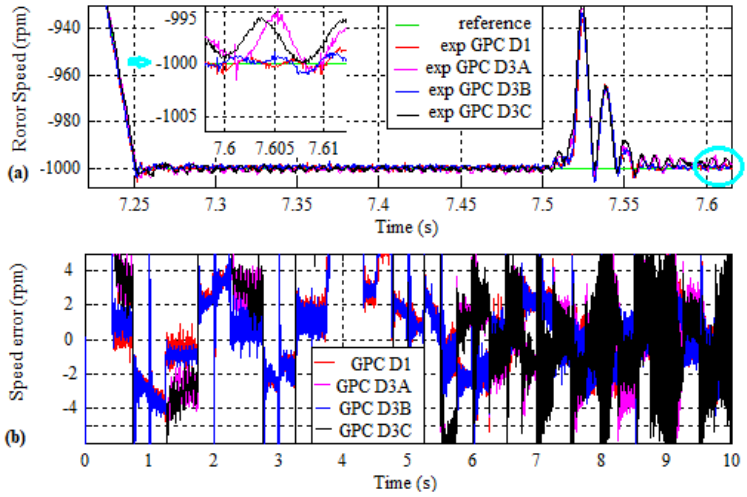

Figure 11: Experimental tests for performance comparison between D1, D3A, D3B and D3C, GPC controller designs.

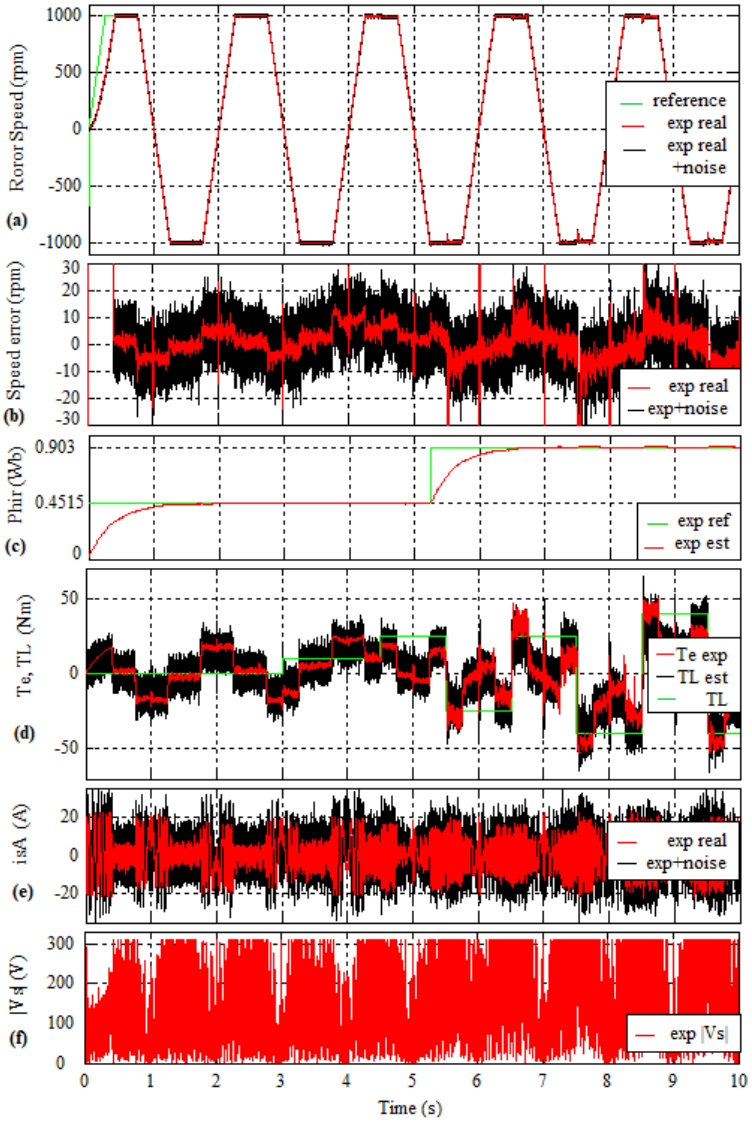

Figure 12: Experimental test of the GPC regulator for induction motor with load disturbance, parameter uncertainties (D3C with D2R design) and measurement noise in the two feedback signals.

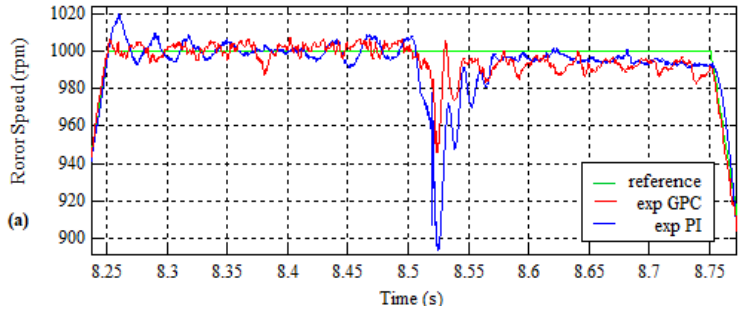

Figure 13: Experimental tests for performance comparison between GPC and PI regulators for induction motor in nominal conditions (D3C with D2R design).